ASCEND
November 16-18, 2020, Virtual Event
ASCEND 2020

10.2514/6.2020-4109

Autonomously Deployable Tower Infrastructure for Exploration and Communication in Lunar Permanently Shadowed Regions

Caleb Amy[1], Marc-André Bégin[2], Becca Browder[3], Manwei Chan[4], Charles Dawson[5], Paula do Vale Pereira[6], Travis J. Hank[7], Eric Hinterman[8], George Lordos[9], Benjamin Martell[10], Alex Miller[11], Cormac O'Neill[12], Vineet J. Padia[13], Natasha Stamler[14], Jessica Todd[15], Nieky Wang[16], Dava J. Newman[17], Olivier L. de Weck[18], Jeffrey A. Hoffman[19]
Massachusetts Institute of Technology, Cambridge, MA 02139, USA

NASA is interested in characterising and robotically exploring the lunar permanently shadowed regions (PSRs) in advance of Artemis crewed landings. The challenging terrain of these regions means a lander would only be able to access the rim of a PSR, limiting line-of-sight communication and sensing into the PSR. Autonomously deployed lunar tower infrastructures could provide valuable lines of sight into and around these PSRs. NASA has developed deployable composite booms for use in microgravity, and we propose an extension of those capabilities by deploying a composite boom vertically in the lunar gravity field. Services hosted by the elevated platform at the top of the boom, such as power beaming, radio repeaters, or imagers, could support the near-term operations of multiple distributed, mobile, robotic assets as well as long-term regional operations of exploration crews. The

[1] PhD Candidate, Dept of Mechanical Engineering, AIAA Student Member
[2] PhD Candidate, Dept of Mechanical Engineering, AIAA Student Member
[3] MS Candidate, Dept of Aeronautics and Astronautics and Technology & Policy Program, AIAA Student Member
[4] PhD Candidate, Dept of Aeronautics and Astronautics, AIAA Student Member
[5] MS Candidate, Dept of Aeronautics and Astronautics, AIAA Student Member
[6] PhD Candidate, Dept of Aeronautics and Astronautics, AIAA Student Member
[7] MS Candidate, Dept of Aeronautics and Astronautics, AIAA Student Member
[8] PhD Candidate, Dept of Aeronautics and Astronautics, AIAA Student Member
[9] (Team Lead) PhD Candidate, Dept of Aeronautics and Astronautics, AIAA Student Member
[10] MS Candidate, Dept of Aeronautics and Astronautics, AIAA Student Member
[11] Undergraduate Student, Physics and EECS, AIAA Student Member
[12] MS Candidate, Dept of Mechanical Engineering, AIAA Student Member
[13] Research Scientist, Dept of Mechanical Engineering, AIAA Member
[14] Undergraduate Student, Mechanical Engineering and Urban Planning, AIAA Student Member
[15] PhD Candidate, Dept of Aeronautics and Astronautics and Woods Hole Oceanographic Institute, AIAA Student Member
[16] Undergraduate Student, Mechanical Engineering, AIAA Student Member
[17] Apollo Professor of Aeronautics and Astronautics, Dept of Aeronautics and Astronautics, AIAA Fellow
[18] Professor of Aeronautics and Astronautics and Engineering Systems, Dept of Aeronautics and Astronautics, AIAA Associate Fellow
[19] Professor of the Practice of Aeronautics and Astronautics, Dept of Aeronautics and Astronautics, AIAA Member

Multifunctional Expandable Lunar Lightweight, Tall Tower (MELLTT) design, created by our interdisciplinary team of MIT graduate and undergraduate students in October 2019, has been selected and funded by NASA STMD and Space Grant as a finalist in the National Institute of Aerospace's NASA BIG Idea 2020 Challenge and will be demonstrated at the virtual BIG Idea Forum in January 2021. The expected result of this work is a proof-of-concept of a TRL 4 prototype of a deployable, tall lunar tower by January 2021, setting the stage for future development along a path to flight targeting an early 2020's lunar tower technology demonstration mission in support of the Artemis program.

I. Introduction and Paper Summary

The environment inside lunar polar permanently shadowed regions (PSRs) challenges robotic and human explorers with extreme cold, extended darkness, ice as hard as basalt, challenging terrain, hard vacuum, and the limited, if not non-existent, line-of-sight communications into or out of the PSRs. Taking advantage of the relatively weak lunar gravitational field and the lack of an atmosphere, a tall, lightweight, autonomously deployed tower, situated just outside the PSR, would provide multiple lines of sight to the Earth, the Sun, the lander, the surface inside and outside the PSR and the distant lunar horizon. Payloads at the top of the tower, up to 16.5 m above the lunar surface, could include radio repeaters and remote sensing, imaging, and power beaming systems.

A lightweight, self-deployable tower infrastructure will aid NASA in achieving the goals of the Artemis program by enabling the exploration and development of PSRs near the lunar poles. The capabilities designed into the Multifunctional Expandable Lunar Lightweight Tall Tower (MELLTT) are key enablers for small, distributed payloads and autonomous robots that operate synergistically to deliver a robust capability to explore and operate in and around PSRs. This aspect of MELLTT has been studied by graduate students at MIT who envisioned a lunar PSR exploration ecosystem supported and enabled by MELLTT.

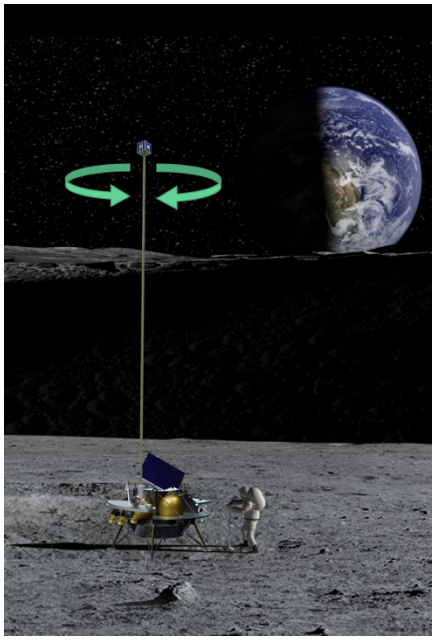

Fig. 1 A rendering of a lightweight tower deployed from the deck of an Astrobotic lander next to a permanently shadowed region near the lunar south pole, with an astronaut for scale. The payload deck at the top of the mast can support a variety of payloads and provide them with lines of sight into the permanently shadowed region as well as the distant lunar horizon

This paper describes the design and development from TRL 1 to 4 of MELLTT. The MELLTT project began in October 2019 and will culminate in a TRL 3/4 demonstration in January 2021. MELLTT has been selected and funded as a finalist by NASA's BIG Idea 2020 Challenge, which is organized by the National Institute of Aerospace. In an effort to demonstrate a proof of concept (non-space rated prototype), a Preliminary Design Review was conducted on

April 27th, 2020. The review demonstrated that the current MELLTT design closes within the BIG Idea Challenge's size, weight and power limitations for a deployable tower that can elevate a 5kg payload to a demonstration height of up to 16.5 m above the lander deck. Due to COVID-19, a planned loan of a 16.5 m composite boom from NASA Langley Deployable Composite Booms team did not proceed as planned. For the purposes of the first prototype, a commercially purchased 6 m composite boom of a different design has been procured and will be integrated with the deployer and payload hardware.

Ongoing component and system testing of this prototype includes physical and power performance analysis for both deployment and operation. The tested operations include leveling the deployer, raising the tower, static loading, slow rotation of the elevated platform, powering and controlling payloads, interacting with remote assets and transmitting and receiving data.

As of the time of writing of this paper, the fabrication and integration of all subsystems is in progress, targeting a January 6-8 2021 demonstration at the virtual BIG Idea Forum. Starting from a tilted mock lander deck, MELLTT will self-level, gradually deploy the boom to full height, and demonstrate nominal operations of the elevated platform. The demonstration payload will consist of a solar-powered radio repeater and a multispectral imager integrated within a 1U Cubesat capable of rotating to a desired azimuth, indicating how the operational capabilities of other robotic assets within and near the PSRs can be enhanced and supported by MELLTT.

The design, development, testing and planned demonstration described in this paper comprise the first phase of a complete path-to-flight strategy for the MELLTT architecture. The development plan includes component, functional, and simulated surface operations testing to verify the proposed system design, aiming for readiness to support near-term lunar technology demonstration missions with as-yet unfunded flight designs that have been proposed to NASA. The MIT team is collaborating with the NASA Langley Deployable Composite Booms team as well as industry partners via proposals to NASA for lunar deployable towers.

II. Problem Statement

In the lead-up to the planned Artemis crewed landings, a fundamental, early-term need for NASA and its international and commercial partners will be to robotically explore and understand the challenging environments in and around PSRs, both from the perspective of science and from that of In-Situ Resource Utilization (ISRU) to support human exploration. Longer term, human explorers at the lunar south pole will benefit from regional area networks that support their needs for high-bandwidth data, situational awareness, and navigation. It is envisioned that these towers and/or the supported assets may be fielded by space agencies or private companies, placing importance on simple, universal interfaces.

As such, the initial goal of the MELLTT project is to chart a path to flight for an initial deployable tower capable of providing a range of supporting services - power, data, situational awareness - to small robotic assets operating in and around the lunar PSRs. From these needs and goals, a set of system functional requirements has been developed, as shown in Table. 1:

Table. 1 System Functional Requirements

ID	System Functional Requirement	Justification
S01	The system must provide Lines of Sight between third-party payloads on the upper platform and the interior of the PSR, the surroundings and/or other deployed assets as needed.	This is the main functional deliverable of the system. Multiple lines of sight meet at the top of the tower and support science and exploration by an ecosystem of small, deployed robotic equipment.
S02	The system must provide third-party payloads fixed to upper platform with launch mount, power, data, pointing, sun sensing, leveling and situational awareness.	The upper platform provides standardized services to payloads with a view to reducing payload size, cost and development time.
S03	The system must meet SWaP and volume constraints appropriate for the selected CLPS lander demonstration in 2023 timeframe.	Selection of CLPS lander provider is assumed.

S04	This technology demonstration system shall utilize flight proven equipment wherever possible	To shorten the path to flight and meet the 2023 launch goal.
S05	The system shall operate for at least 14 days.	To match or exceed the expected life of near-term CLPS landers.
S06	The system shall return engineering data suitable for the validation of the current design and for designing the next generation of towers.	Data from the landing, deployment and operations phases of the first prototype tower and demo payloads will inform the design of taller, larger towers that can support more advanced payloads.

Based on these system requirements, and on principles for landing site selection, the team was able to proceed with the detailed design of the first MELLTT prototype, which will be described below

III. Landing Site Selection

This project aims to elevate payloads up to 16.5 m above the lunar surface to provide the payloads with a line-of-sight into PSRs. An appropriate landing site must thus be selected to enable this line-of-sight into the area of interest from the desired height above the landing site surface. Additionally, the landing site must have a tilt of less than 20 degrees to ensure MELLTT is able to be leveled.

Using data from the Lunar Orbiter Laser Altimeter, the team developed an interactive tool for screening potential landing sites that shows which areas of the lunar surface are visible from a tower placed at any point between latitudes 80°S and 90°S. This region was identified as the bounds for landing sites because 90°S delineates the south pole and 80°S is the extent north of the pole where high-resolution data is available. The 80°-90° area also approximately corresponds to where the majority of south pole PSRs are, and the tool can be easily extended to other regions where topographical data are available if needed. This tool can be shared in order to work with NASA and the CLPS provider to select a final landing site.

Using these considerations, two potential landing sites were identified. Fig. 2 shows the location of a potential landing site near Slater crater. This landing site is situated in a partially-illuminated region on the floor of a large (>10 km diameter), flat depression near Slater crater, which provides easy visibility into a large PSR. Two disadvantages of this site are the lower average surface temperatures and lower illumination within the site compared to most other craters.

Near the Cabeus and Haworth craters lies a second candidate site (Fig. 3), which contains two areas that are likely PSRs. This landing site has the benefit of being relatively flat and being outside of a crater, providing a larger window of illumination during the lunar day. Drawbacks of this site include partially obstructed visibility into the smaller PSR, and completely obstructed visibility into the larger PSR, given the location of the landing ellipse and the height of the MELLTT tower.

For MELLTT, the Slater candidate would be a better landing site because of the increased area of the PSR inside the field-of-view. However, keeping in mind that other payloads with different landing site requirements will fly on the same mission with MELLTT, the candidate site identified in Fig. 3 would also be acceptable.

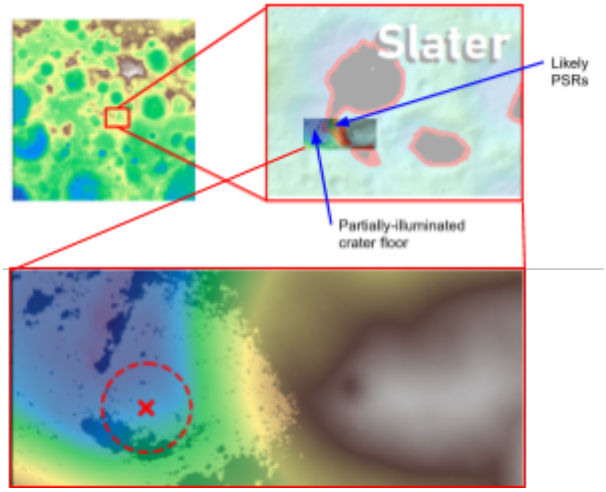

Fig. 2 A potential landing site adjacent to Slater crater. In the lower map, the candidate landing site is shown as the red marker, and the lighter regions indicate regions with line-of-sight visibility to a tower at the landing site. A much greater portion of the PSR is visible from this landing site than the site depicted in Fig. 3

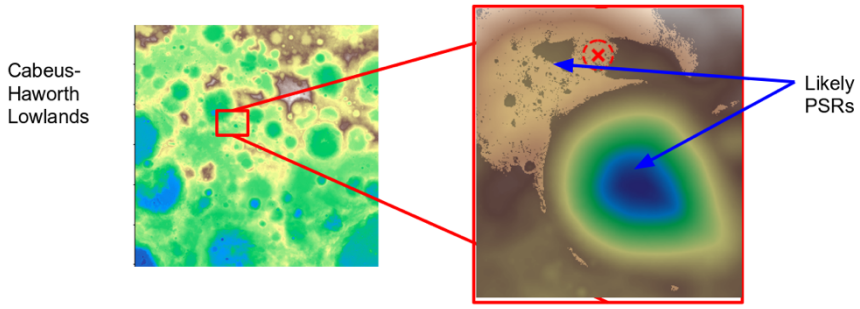

Fig. 3 An evaluation of a potential landing site in the lowlands between Cabeus and Haworth craters. The red marker in the inset shows a candidate landing site, and the light brown overlay shows the regions within line-of-sight of a 30m tower at the landing site. This analysis reveals that the larger PSR is completely obstructed by the crater rim, while the smaller PSR is partially visible.

IV. System Description

A. Design Overview

The first MELLTT tower prototype is designed around a space proven, lightweight bi-stable carbon-fiber composite boom that is rolled flat on a spool and takes the shape of a rigid cylindrical mast upon unspooling [4,5]. A leveler subsystem aligns the deployer subsystem with the lunar gravity field, and a self-powered elevated payload platform at the top of the composite boom hosts the imaging and communications demonstration payloads. Together, these subsystems make up the MELLTT system, which is shown in Fig. 4. A photogrammetry experiment mounted on the leveler base collects engineering data during deployment and operations, informing the iterative design of future generations of lunar towers.

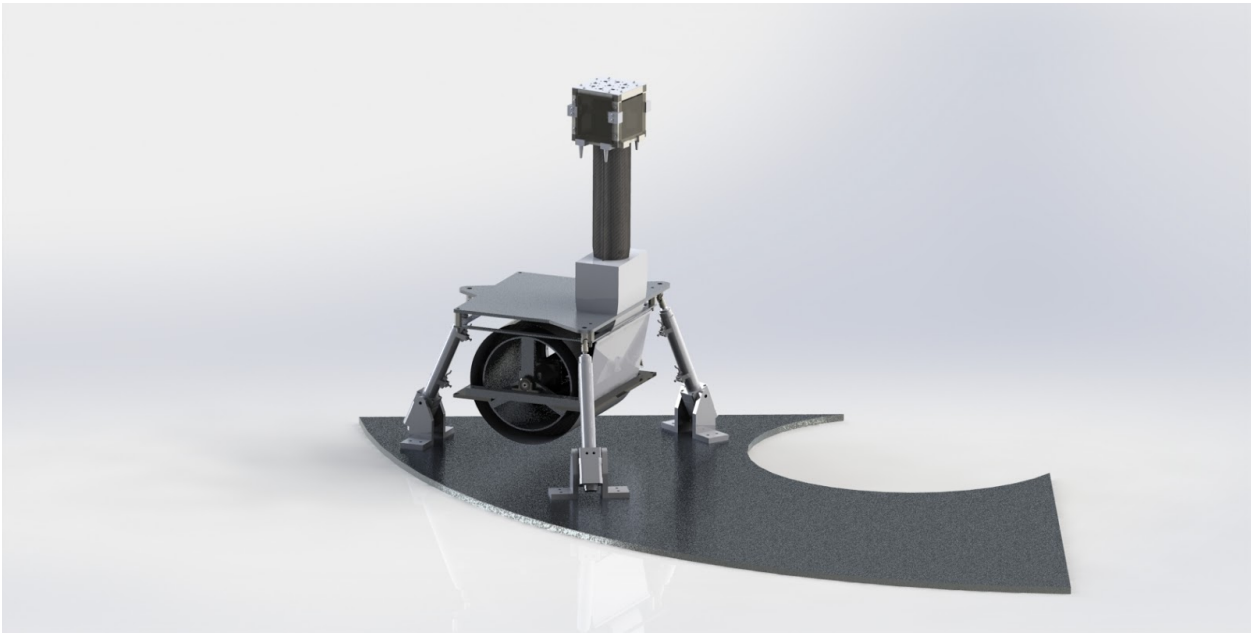

Fig. 4 A close up rendering of the base of the MELLTT tower showing the lander deck, leveling actuators, deployer subsystem, the partly-deployed composite boom and the 1U CubeSat demonstration payload.

B. Elevated Platform Functions and Services

Anticipating the need to cater to many applications, lower costs and raise the TRL at component level for faster deployment by building on proven heritage space hardware, the elevated payload platform in the MELLTT concept is a CubeSat, offering "plug and play" services of standard mounting, power solutions and data interfaces to a range of hosted payloads that can benefit from the multiple lines of sight. The avionics and communications system provide plug-and play data, control, and telemetry services to the elevated payloads. In addition, MELLTT's elevated platform and its client payloads will be independently powered by fixed solar cells on all four vertical sides of the CubeSat which provide simplicity and security of power supply to the payloads. This power source will also supply an actuator to rotate the platform, delivering an azimuthal pointing capability, useful to payloads such as imagers and high gain antennas. The initial MELLTT prototype features a 1U CubeSat, as shown in Fig. 4.

C. Lunar Infrastructure Functions and Services

By deploying MELLTT towers near a PSR exploration zone, future missions to the same region can enjoy increased operational capabilities at reduced costs. The accumulated MELLTT infrastructure supports the improved range and reliability of regional surface communications, stereoscopic mapping and real-time situational awareness in the vicinity of landers, identification of potential routes into or out of a PSR, wireless energy transfer in the form of reflected sunlight, microwaves or lasers, and more. MELLTT's elevated payload platform benefits any payload that can use its high vantage point, multiple lines of sight, plug-and-play power, and data and pointing services. With future lunar infrastructure functionality in mind, MELLTT is being designed from the outset with a view to a future capability to outlive its host lander. The leveler's locking mechanism is passive, requiring no power from the lander to hold its leveled pose, and due to the oblique angle of incidence of sunlight at the lunar pole that makes some high-elevation regions experience near-constant illumination, solar panels at the top of the tower may be more consistently illuminated than panels on the lander. This could allow the elevated payload platform to capture energy with which to continue providing services to nearby assets, turning older towers into longer-lived infrastructure that forms part of an expanding regional network.

D. Tower Subsystems

1. Tower Structure Subsystem

The tower structure is based on a flight-heritage deployable composite boom concept that has been used in microgravity situations on board satellites. These booms are typically stored rolled up flat in a spool during space travel. Once the desired location is reached, the spool unravels, deploying a straight boom that naturally takes its shape. These composite booms can take many different cross sectional shapes, the most common being the C-shaped

boom. MELLTT is testing both a C-shaped boom with a slit-lock technology, as well as a lenticular shaped (double-omega) boom. Neither of these types of booms have been tested in lunar gravity before. The main objective of this study is to determine the feasibility of using deployable composite booms in gravity to support a payload at the top. Some analysis has been done, however, the main contribution that the authors hope to provide is experimental testing of the performance of the booms in gravity.

2. Deployment Mechanism Subsystem

The deployer design is shown in Fig. 5 a) and is based on a tube that is unspooled by a motor to push the boom through a bracing system, which supports it during transition from a flat to a deployed shape. The motor and gearbox were sized to provide approximately 5X the estimated torque required to overcome Earth's gravity and friction.

The deployer includes two types of bracing. As the boom is unspooled, blossoming is prevented by a low friction surface held tightly around the boom by springs. To prevent buckling due to the gravitational loads during the boom's transition from flat to lenticular, a fully-enclosed 3D printed structure shown in Fig. 5 b) lends significant support, with an additional goal of low friction operation.

An additional deployment system is also being developed, which pulls the boom out rather than pushing it. This powered system, depicted in Fig. 5 c), is situated at the top of the bracing mechanism and grips the flat edges of the double-omega boom, helping to hold the weaker section of the boom beneath it in tension.

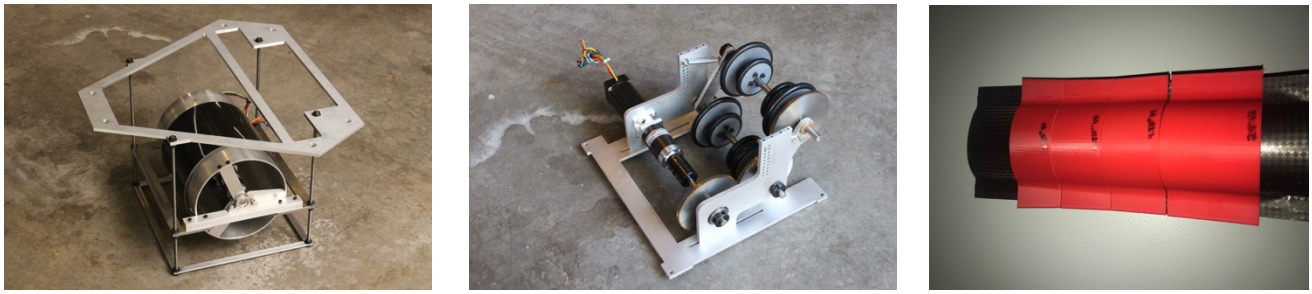

a) **b)** **c)**

Fig. 5 a) The deployer pusher subsystem in development, with a permanently-flat testing boom installed. b) The deployer puller subsystem in development, depicted in stowed position. The boom goes through the two sets of high-friction rollers on the right. c) Upper brace prototyped as several 2-3 inch 3D-printed sections.

3. Self-Leveling Base Subsystem

The tower deployer is mounted onto a dynamic base capable of levelling the tower with the use of a sensing and actuator system. Given the full height of the tower at 16.5 m, a small deviation in incline at the base would create

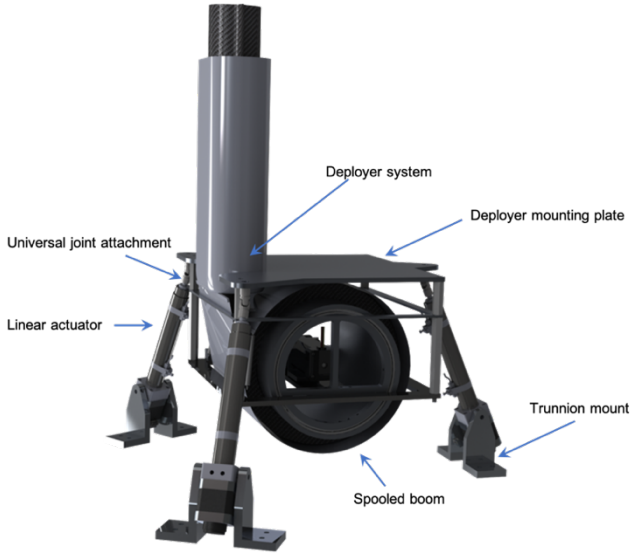

Fig. 6 CAD rendering of the self-leveling tower base.

create a large moment arm and risk tipping or warping the tower. This self-leveling base has three primary functions: (1) align the tower with the lunar gravitational field to account for any incline in the terrain of the landing site, (2) compensate for any shift in lander or tower position caused by deployment of other payloads, moonquakes or other vibrations or shocks, and (3) allow the angle of the deployed tower base to be adjusted to account for boom bending. The leveling system design is a modified Stewart platform consisting of a mounting plate supported by three linear actuators attached with universal joints. These actuators are mounted directly onto the lander platform with trunnion mounts, providing hinge action. The actuators can adjust the platform in two degrees of freedom (roll and pitch) to achieve leveling of up to ±20°. The team anticipates that commercial lunar landers will not attempt to land on slopes greater than 20°. The deployer is mounted into the leveling plate as shown in Fig. 6. These linear actuators are controlled using stepper motors.

The system uses Tinkerforge accelerometer units, consisting of three-axis accelerometers integrated into a single chip, mounted onto the leveler plate, lander platform and payload platform, to determine the orientation of the tower relative to the gravity gradient. Forward kinematics use this sensor data to determine the current pose and attitude of the leveling platform. Inverse kinematics are used in real time to determine the required linear actuator extensions for the desired platform pose and attitude. Further details of this process can be found in Appendix A.

When powered off, the leveling system remains locked in position. To avoid resonance or unwanted vibrations in the tower, the leveling system does not continually actively level the system during deployment and operation. The tower base is designed to actively self-level at fixed intervals during the deployment phase, as discussed in the concept of operations, as well as enabling manual leveling via operator input. The accelerometers remain active during operation to detect any change in inclination or boom bending, at which point the leveling system can be switched on to actively level if an incline is detected.

4. Elevated Payload Platform Subsystem

To provide client payloads with access to the benefits of an elevated vantage point (e.g. allowing the line-of-sight to be extended over ridges and cusps, increasing the overall line-of-sight footprint, more frequent solar power availability, etc.), the MELLTT system includes a payload platform mounted to the top of the tower. In the current design, this platform is modelled on a 1U CubeSat with exterior solar panels on the four sides and a top deck with mounting holes (Fig. 7 a)), with most of the interior volume taken up by the pointer motor, battery and avionics packaged as shown in Fig. 7 b). The primary function of the elevated payload platform is to provide a standardized interface for mounting client payloads, provide power and communications services to those payloads, and provide azimuthal pointing for payloads. Our use of the CubeSat form factor allows us to leverage the broad range of readily available space-heritage CubeSat hardware, shortening the path to flight for this subsystem while increasing its reliability and standardization.

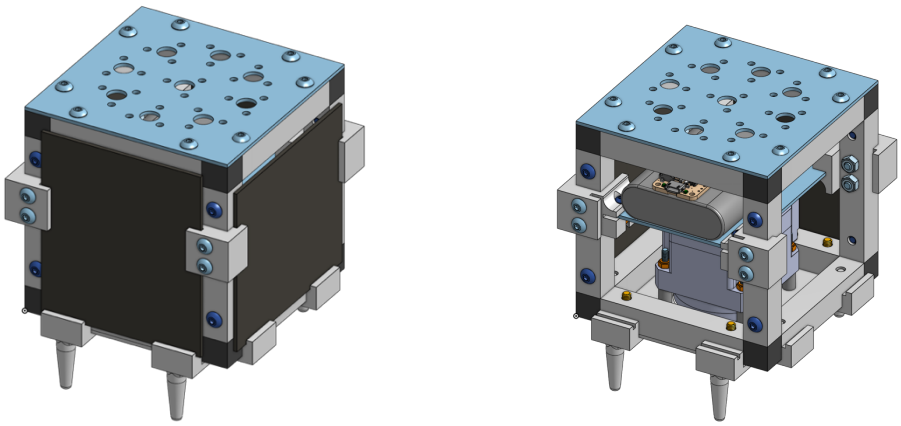

a) **b)**

Fig. 7 a) The 1U payload platform, with standardized mounting for client payloads on the upper surface of the platform. b) Interior packaging arrangement showing pointer motor, battery and avionics. The client payloads in this design iteration are hosted on the top deck.

The azimuthal pointing capability is provided by an internal servo motor, which is used to rotate the entire payload platform about the long axis of the boom. The choice to rotate the entire platform, rather than just a portion of it, was based on the need to carefully control the location of the center of mass of the platform with respect to the center of the boom to ensure that the center of mass does not shift away from the base of support during operation. Additionally, the ability to rotate the solar panel assembly as well as the individual client payloads provides redundancy, since solar tracking can be employed to compensate for the potential loss of up to two solar panel arrays. The payload platform includes internal command and control subsystems that determine the target orientation of the platform, negotiating between power-generation considerations and requests from individual client payloads.

The payload platform includes self-contained power and communications subsystems to provide power and communication services to the client payloads,. The communications subsystem contains two radio transceivers. The first is a short-range WiFi link for communicating between the payload platform and the lander (which can then relay data back to Earth). The second is a 1W 900 MHz ISM band transceiver capable of creating a mesh network with nearby towers and with rovers exploring within the PSR (which would otherwise be occluded by the crater rim).

The CubeSat includes a power generation (solar cells) and storage (batteries) subsystem that is completely isolated from the lander and tower-base power systems, to power the radios, as well as to provide power for client payloads and platform rotation,. The isolation of the payload platform power subsystem means that the payload platform is potentially capable of surviving the death of the lander during the lunar night, since the elevated platform will have access to solar power further into the lunar night due to the high angle of solar incidence at the lunar poles. The platform power subsystem includes a lithium polymer battery with 22.2 Wh storage capacity, four solar panels mounted around the outside of the platform with 2.7 W combined generation capacity, and charging and distribution components producing regulated 5 V and 12 V power buses. In the nominal 1U design, we maintain a 5:1 ratio of charging time to operation time in the maximum power configuration, but this ratio can be improved by operating below maximum power (i.e. duty-cycling the high-power long range radio). Larger configurations (such as 27U or 1U with fold-out solar panels) can also achieve smaller charge to operation ratios through increased power generation capacity. In the 1U variant, client payloads are expected to provide independent thermal management systems, since they are mounted on the exterior of the platform; in the 27U variant, we create a “warm-box” environment for client payloads mounted on internal payload racks.

5. *Command and Control Subsystem*

The control system is constructed in the Robot Operating System (ROS) framework which provides a simple method to interface subsystems through standard messaging for sensors and actuators. Fig. 8 summarizes the logical components along with their physical or software interfaces.

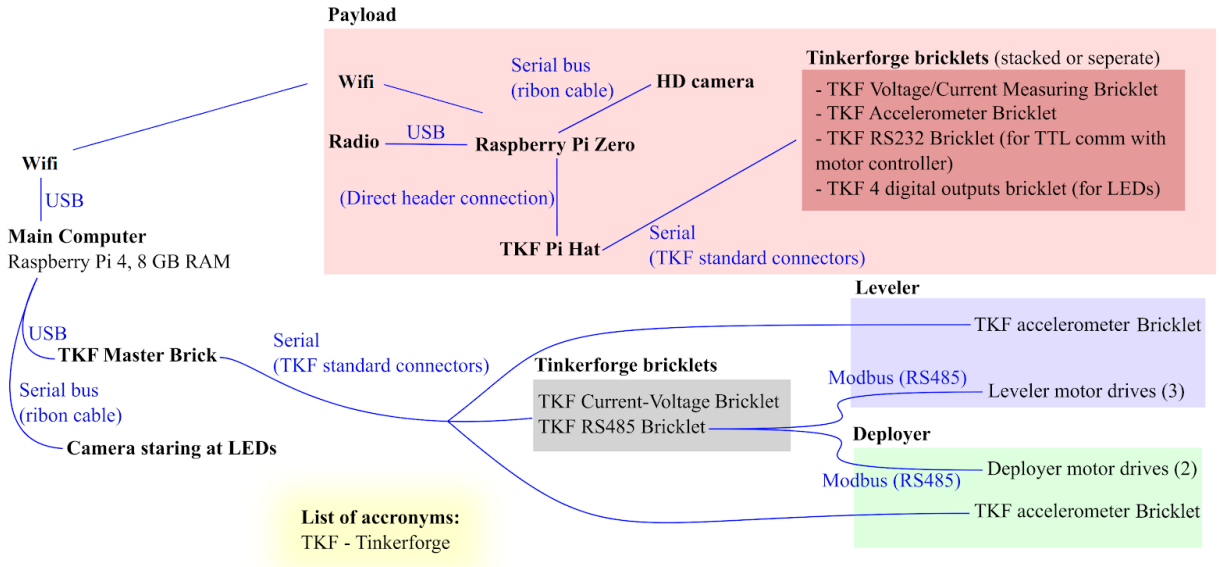

Fig. 8 System diagram of logical components and their interfaces.

Onboard the elevated platform subsystem, a Pi Zero computing module is used to capture images from a servo-articulated camera, thereby enabling high resolution panoramic footage. In addition to visual data, the acceleration of the elevated platform is measured. This measurement provides redundancy for computing the gravity vector for leveling and also facilitates measurements of boom movement and vibrations. The images and acceleration data received from the payload are transmitted via a short-range WiFi link to the lander.

To better assess the static deflections of the elevated platform, a monocular photogrammetric method has been implemented to estimate the platform pose [6], consisting of a high definition camera on the lander with an IR-Pass filter to image four infrared LEDs that are installed on the bottom surface of the platform. Four LEDs were chosen because the full pose of the payload can be reconstructed by tracking the distances between the LEDs. The IR-Pass filter in combination with IR LEDs is an effective method to increase the contrast of the images and prevent background noise.

In both the lander and elevated platform, power diagnostics are important to prevent damage by monitoring power from the solar panels and power supply. The MELLTT system has the ability to actively sense both the current and voltage, and minimize failure by shutting down problematic components.

Within the leveling and deploying subsystems, third-party motor controllers are used to implement closed-loop control of the motor position and velocity. By using the daisy-chain property of Modbus RTU communication protocol, a single Tinkerforge RS485 Bricklet is used as a Master device to interface to the system specific motor controllers. In both the deployer and leveler subsystems, Tinkerforge accelerometers are used to establish the gravity vectors. This information is streamed to the main computer, a Raspberry Pi 4B, which computes the current and desired pose of the leveling system. During the deployment phase, the internal state machine oscillates between incrementally deploying the boom and releveling the leveling subsystem. This prevents the tower from suddenly becoming unstable and ensures a steady controlled tower deployment.

6. CLPS Lander Constraints

The constraints of the BIG Idea Challenge included designing a payload that could be integrated onto a NASA CLPS lander[20] using Astrobotic's design and Payload User Guide[21] as an example. This included restrictions on mass, power, and communications. The main CLPS constraints applicable to the MELLTT design were:

Power

I. At least 8 W continuous and 40 W peak for 5 minutes
II. Regulated and switched 28Vdc

Communications

I. Bandwidth (rate at which data can be sent to the lander): At least 70 kbps per kg of payload (if more is needed, internally store/buffer to stay under 70 kbps)
II. RF comm (rate at which comm can be relayed to Earth): 70 kbps per kg max (if more is needed, internally store/buffer to stay under 70 kbps)
III. Wireless comm: 2.4 GHz IEEE 802.11n compliant WiFi

In addition to these constraints on power and communications, the team added another constraint based on CLPS capabilities: the ability to level the system. While CLPS providers appear to be designing leveling systems into their landers in order to accommodate landing on a slope on the lunar surface, being level is critical for MELLTT's tower deployment, so a system leveler was also designed. Based on a literature review, the team determined that the system should be able to level up to 20° to accommodate a wide range of landing locations on the Moon. In the event that the CLPS leveling works but is not sufficient to achieve perfect leveling, the MELLTT system will be able to provide the final leveling needed. The MELLTT leveler also provides redundancy in case the CLPS leveling fails.

In order to make this phase of the MELLTT design as close to a flight-ready version as possible, a mock lunar lander was constructed to address the three constraints described above: power, communications and leveling. The mock lander will house the main power system and the main computer, will allow for testing of the MELLTT leveler, and will provide a platform to support MELLTT. In order to test the MELLTT leveler, an extra feature was designed into the mock lander: a movable platform that allows the entire system to be tilted. Fig. 9 shows the CAD design of this mock lunar lander.

[20] http://bigidea.nianet.org/competition-basics/
[21] https://www.astrobotic.com/configure-mission

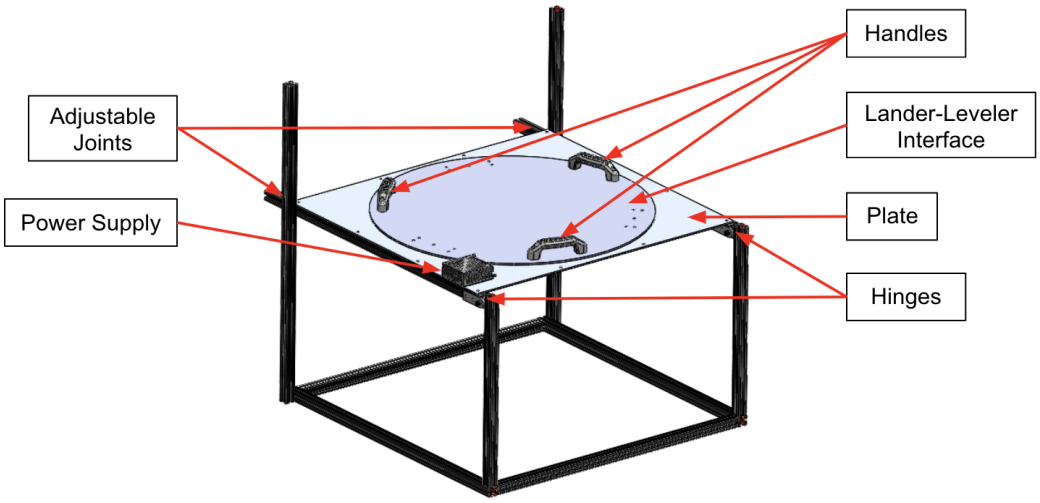

Fig. 9 CAD of the MELLTT mock lunar lander with callouts identifying components.

The mock lunar lander houses the main power supply for the MELLTT system and will also house the main computer, both of which are designed to meet the CLPS constraints. The mock lander has hinges and adjustable joints that allow the platform to be tilted in a single direction, enabling testing of the leveler subsystem at various slopes. The lander-leveler interface sits on top of the plate and the plate can be rotated, allowing the leveler to be tested at slopes in multiple directions. Handles are attached to the lander-leveler interface for ease of adjusting the system.

7. Mass, Power and Link Budgets

The power budget for the elevated platform of this demonstration system is 1.4W, which is the average production of the 1U CubeSat solar panels. The link budget for a 1W radio closes over 5km with 6dB margin. As currently designed, MELLTT will have a total system mass of approximately 25 kg. A breakdown of the mass budget by subsystem can be found in the Appendix.

8. Earth Proof of Concept Test Plan

For the Earth proof of concept design, the project team developed a test plan with four phases as shown in Fig. 10:

1. Test for interfaces
2. Test for Earth proof-of-concept
3. Test for launch and flight
4. Test for surface operations

Phases 1 and 2 were planned as part of the BIG Idea project, with phases 3 and 4 left for future development to bring the payload to flight readiness. While phase 1 testing is in progress, continued COVID-19 lab restrictions at NASA and MIT have prevented the team from pursuing phase 2 tests. In order to achieve our minimum viable product, which includes a demonstration of the Earth proof of concept, the team plans to complete phase 1 testing. At this point, it is uncertain whether the team will be able to conduct any of the phase 2 tests which would lead to TRL 4.

However, by completing phase 1 testing, MELLTT will achieve TRL 3, "analytical and experimental critical function and/or characteristic proof-of-concept"[22]. The MIT team is pursuing additional funding to continue development, which would leverage phases 2-4 of the testing plan to continue increasing MELLTT's TRL until it is ready for launch.

[22] https://www.nasa.gov/directorates/heo/scan/engineering/technology/txt_accordion1.html

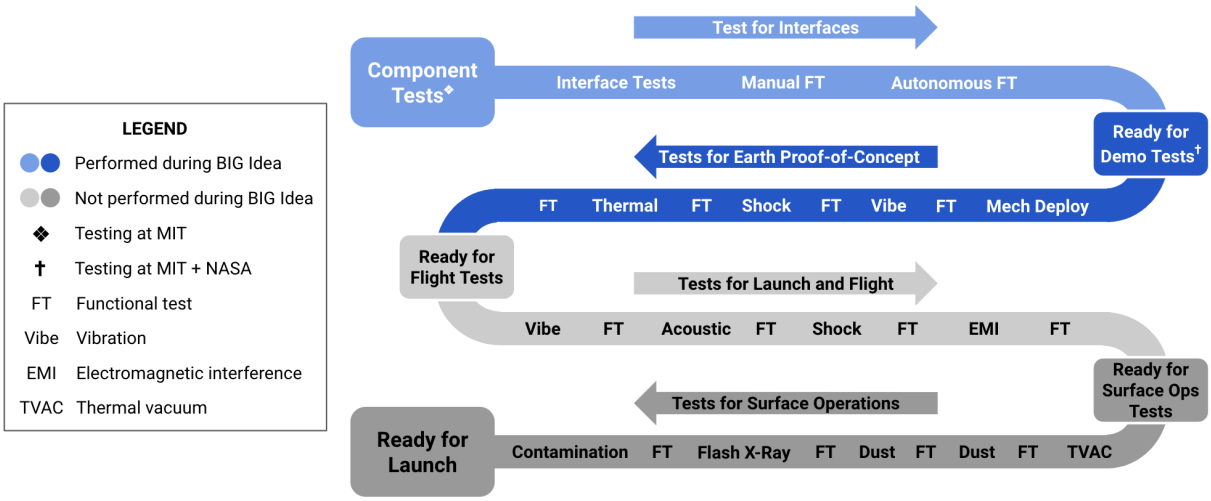

Fig. 10 System test plan including 1) component testing, 2) ready for demo testing, 3) ready for flight tests, and 4) ready for surface operations tests.

9. Risk Analysis and Mitigation

Fifty technical and logistical risk factors were assessed and mitigation strategies considered for each of them. A breakdown of the exact technical risks by subsystem can be found in the Appendix.

V. Lunar Tower Mission Architectures

A. Concept of Operations (CONOPS)

Fig. 11 shows the Concept of Operations for an Earth demonstration of the MELLTT system outlined in this paper. The MELLTT tower is deployed from the mock lunar lander at an initial incline, with the *Deployment* phase lasting several hours as the boom is incrementally deployed and leveled. At full deployment, a full systems check is performed and then each payload system tested.

Fig. 12 shows the Flight Concept of Operations for MELLTT for a lunar-rated system. Following delivery to the lunar surface by a Commercial Lunar Payload Services (CLPS) landing system, MELLTT will be deployed directly from the landing platform. The *Deployment* phase of operations will last approximately 1 Earth day. Initial leveling will take place to account for lander incline prior to deployment. The tower is then deployed and if leveling sensors detect a severe deviation equivalent to a lateral warp beyond approximately 1% of boom length the deployer is halted while the system self-levels. Following full deployment and a full checkout of all subsystems, the *Operations* phase begins, providing a full lunar polar day (13 Earth days) for payload operations. The first lunar demonstration of MELLTT will include camera tests (rotations and stereo image depth sensing), pointing test to test the accuracy of the rotational payload platform and the stability of the tower, and testing of the independent payload deck power system.

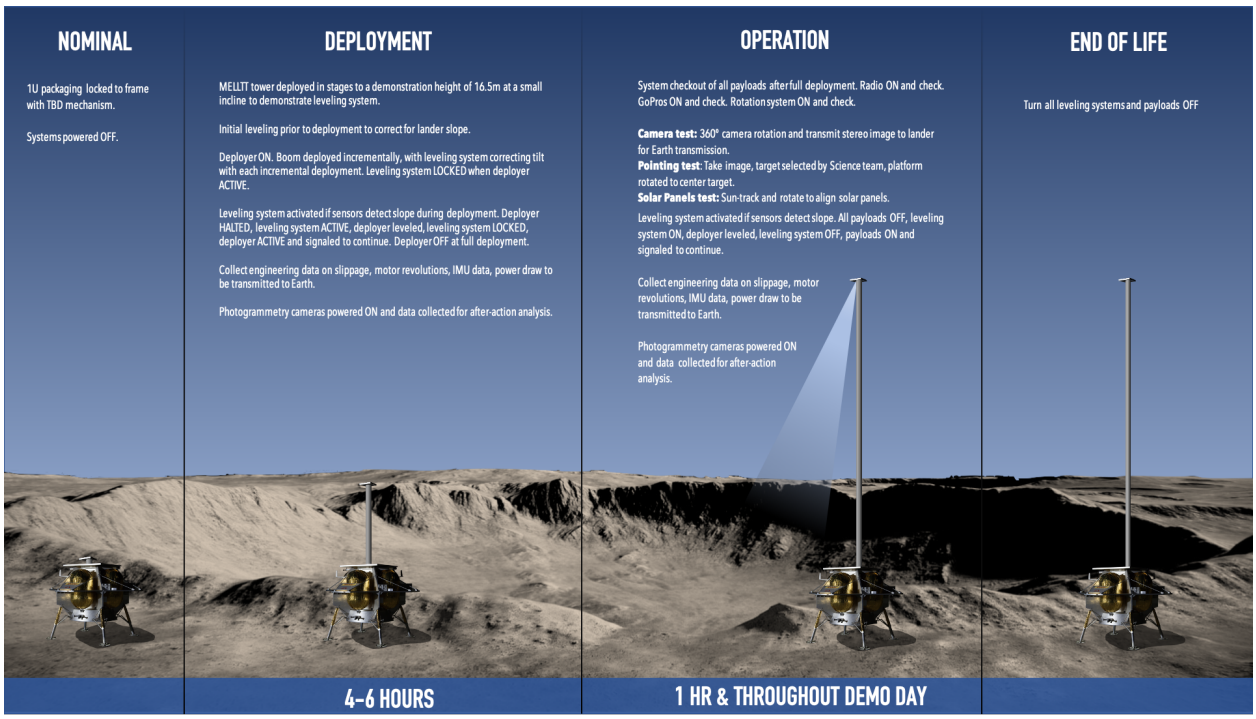

Fig. 11 Concept of Operations for MELLTT Earth Demonstration

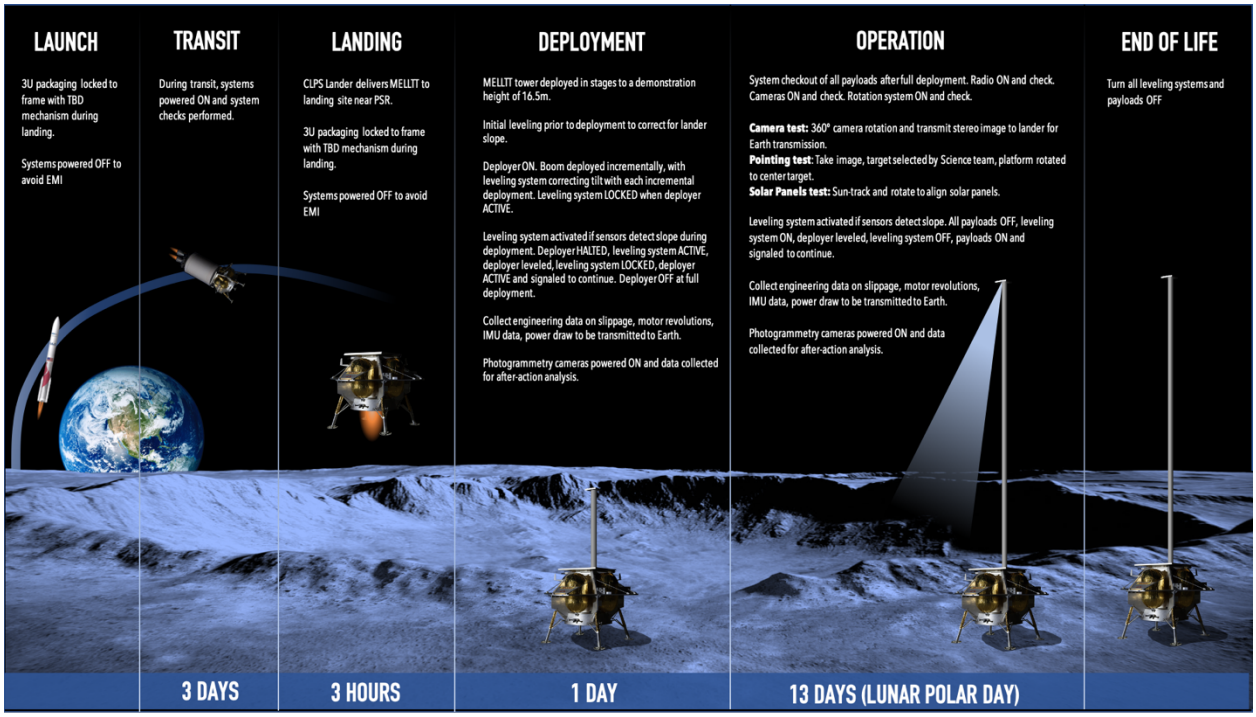

Fig. 12 Concept of Operations for MELLTT on the Lunar Surface

B. Design Variants

1. 27U Tower Variant

A more capable design based on a 27U Cubesat has been created in collaboration with NASA Langley's Deployable Composite Booms team and proposed to NASA as part of the PRISM RFI call. This design is shown in Fig. 13.

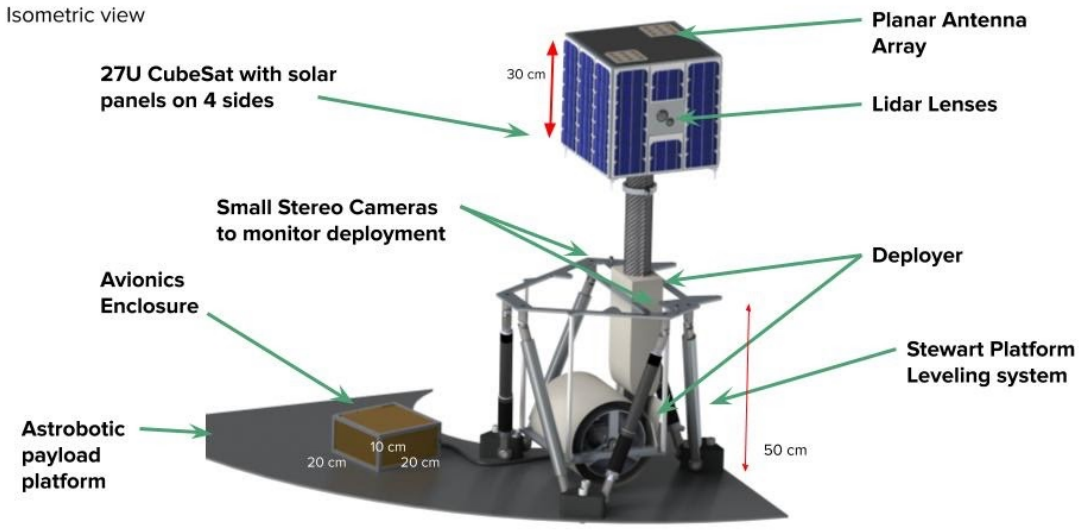

Fig. 13 Higher capability self-erecting lunar tower with instruments (SELT-I) including a 27U payload package and modified leveling system.

2. Networked Towers

Networks of deployable towers have applications for manned and unmanned missions serving both in an individual role or in a networked fashion. Elevated platforms provide direct lines of sight avoiding topography challenges found in non-uniform terrain. If explorations are planned into craters or other natural valley points the platforms can operate as robust, redundant comm relays or power beaming stations. A tower connected to a functional base such as a lander enables extra power and processing to be carried in the base while reducing construction time and complexity. Beamed power can be especially beneficial when exploring polar craters where solar power is not an ideal source. A number of networked applications for the MELLTT concept are explored by Johanson et al in [7].

3. Local Navigation Grid

Multiple towers can act in conjunction with one another allowing for signal relay across long distances. They could act together covering blind spots such as different slopes of a creator. Additionally, utilizing signal triangulation, a local navigation grid can be formed enabling location finding, tracking, mapping, and navigation of manned and unmanned vehicles. Similarly a wide area network could be formed for data relay. A deployable tower when attached to small autonomous landers such as Astrobotic's Peregrine landers can be a scalable affordable option for establishing tower networks for utilization by manned and unmanned systems.

VI. Results and Future Work

A. Results to Date and Expected Results

Given the potential utility and attractiveness of lunar towers described in this paper, the key results targeted by the MELLTT project are related to the technology development of autonomously deployable, lightweight towers with an early flight demonstration as a key milestone. A breakdown by subsystem and by development phase shown in Table. 2 indicates the engineering data coverage that we intend to produce. This data will be fed back into the design process to inform future generations of lunar towers with a goal of continuous improvement in load-bearing capability, reliability, longevity, system mass and tower stability.

Table. 2 Results to date and expected results for the Earth Prototype and for a future TRL8 lunar prototype

Work Package / Subsystem	Results to Date (TRL 2)	Expected Results - Earth Prototype (TRL 4)	Expected Results from Lunar Prototype (TRL 8)
Deployer subsystem	Prototype built as proof of design concept	Characterize frictional forces to overcome; validate ability to deploy reliably	Engineering data on deployer health incl. temperatures, voltages, power draw
Leveler subsystem	Prototype built as proof of design concept	Characterization of precision, accuracy and fine adjustments; validate ability to hold pose without power	Engineering data on linear actuator health incl. temperatures, voltages, power draw
Deployable boom	Bracer and rollers built as proof of concept	Characterization of twisting, warping, oscillations and validation of static load bearing ability	Temperature data; and time stamped engineering data from photogrammetry (pose, distance)
Elevated payload platform	Platform built as proof of concept of design	Proof of concept of nominal operations (powering, imaging, radio, pointing)	Engineering data on: pointing, solar panels, data rates temperatures
Command & Control subsystem	Forward and backward kinematics equations derived	Verification of command, remote control and telemetry	Observe autonomous operations in lunar environment and validate command & control

B. Future Work and Path to Flight

A framework for cataloging the steps in the operating sequence is used to investigate the design changes necessary to convert the Earth prototype being developed for BIG Idea into a flight article. In the majority of cases, the required path to flight change is substitution of hardware with a space-qualified part that accomplishes the same delivered function. In Table. 3 below, red indicates a required path to flight design change while green indicates that the Earth prototype component / operation is largely ready for flight."

Table. 3 Integrated Concept of Operations and Path to Flight Design Changes

Concept of Operations: Stage of Operation	CONOPS Stage Enabled by Earth Prototype System	Path to Flight Design Changes to Support Flight System Operations
Pre-launch integration with lander	Mechanical integration of Earth prototype packaging with a model of a CLPS lander deck	Design/materials to ensure adiabatic thermal interface between payload and lander deck
Survive through launch acoustic environment	Prototype packaging, which will differ necessarily from flight packaging	Integration changes and subsystem swaps; flight hardware acoustic tests
Survive space environment during transit and landing on the Moon (Fig.12, Step 2 & 3)	Functional prototype avionics and initial thermal design appropriate for Earth prototype packaging, to contain costs	Incorporate flight-proven, radiation-hardened avionics and a space-qualified thermal design at higher cost

Post-landing, pre-deployment self-test and diagnostics (Fig. 12, Step 4)	Semi-automated or manual testing and diagnostics	Incorporate flight-tested automation, telemetry and telecontrol
Open cover, carry out leveling operations (Fig 12., Step 4)	Use flight-like active leveler to level deployer within Earth's gravitational field	None/minor software change - easier in reduced gravity environment
Lock the deployer in the level position (Fig. 12, Step 4)	Flight-like locking system capable of withstanding "leaning tower torques" at 1g; test at MIT and NASA facilities	None; flight system will operate in easier reduced gravity environment, but verify thermal performance
Deploy tower to test height (2m) (Fig. 12, Step 4)	Flight-like tower deployment system, deploying vertically to a height of 2m under Earth gravity from simulated lander deck	For boom, none/minor software change (easier reduced gravity environment), but replace deployer motor with a flight qualified model
Perform diagnostics while partially deployed for GO/NO GO full deployment decision	Wireless connection between top deck / deployer avionics; verify tower is vertical with respect to Earth gravitational field	None/minor software change - easier reduced gravity environment
Contingency: tower departs from vertical while deploying	If departure from vertical detected, retract boom, re-level, re-deploy	None/minor software change - easier reduced gravity environment
Deploy tower to 16.5m height (Fig. 12, Step 5) (For deviations from nominal: see contingency)	Flight-like deployment system: slow deployment, monitoring top deck IMU for deviations from vertical	None/minor software change - easier reduced gravity environment
Validate repeater functionality by parroting back lander transmission (Fig 12, Step 5)	Prototype repeater mounted on tower top deck will not be space-qualified	Design/procure and integrate actual flight payloads (repeater, imager)
Perform elevated deck rotation test, validate using imager data (Fig 12, Step 5)	Slowly rotate top deck to deliver pointing / rotisserie service to payload	Replace with a flight-qualified actuator to provide top deck pointing
Contingency: tower departs from vertical while operating	If dynamic departure (swaying), cease operations until oscillation dampens If static departure (bent mast), re-level and restart nominal operations.	Future designs for MELLTT may incorporate active or passive damping systems into the leveling base to address boom vibration / shock.
Return all test data to Earth	Transmit all data from payload to "lander"	Replace with flight data/comms payload

VII. Conclusion

As robots and humans travel to the lunar south pole and begin to explore its Permanently Shadowed Regions, they will face many key challenges that threaten their missions. Among these will be a lack of line-of-sight communications from a sunlit ground station to assets inside the PSR. The Multifunctional, Expandable Lunar Lightweight, Tall Tower (MELLTT) project described here is a novel solution to this problem, enabling important science and exploration missions that may otherwise prove infeasible, too risky or too complex without this proposed tower infrastructure.

Appendix A

The control objective for the leveller is to orient the platform supporting the boom deployer in such a way that a vector normal to the surface of the platform is aligned with the lunar gravity vector. Hence, given the 3-axis

components of the gravitational acceleration as measured by an accelerometer mounted on the base of the moon lander, the leveller controller must first determine the desired leg lengths which will bring the platform in alignment with gravity. Note however that the leveller system has 3 degrees of freedom whereas only 2 degrees of freedom (or 2 legs) would only be needed in theory to level the platform. To obtain a unique solution to this inverse kinematics problem, a simple algorithm is proposed that will always fix the desired leg lengths such that the platform is always at its lowest possible position, thus minimizing the height of the centre of gravity of the system.

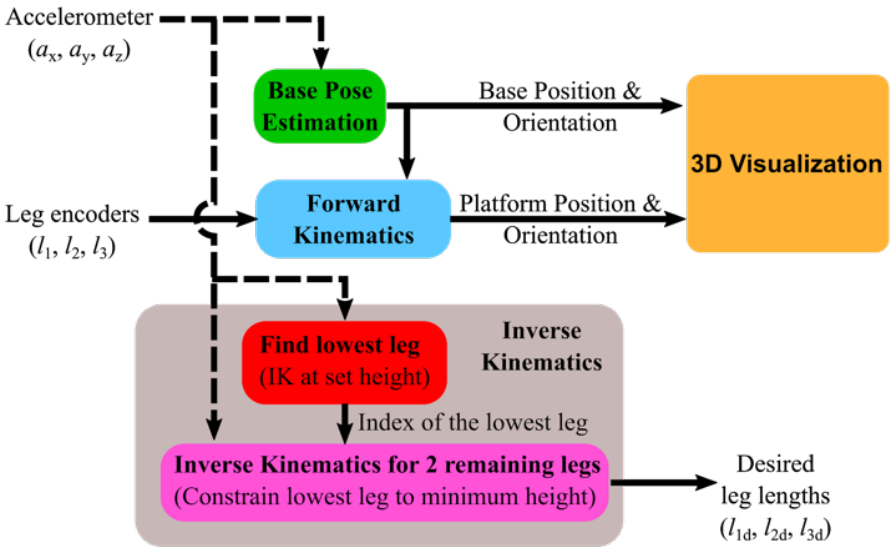

Fig. 14 Pathways for the Forward and Inverse Kinematics of the Platform

The inverse kinematics problem is split into two steps as summarized in Fig. 14. First, an alternative kinematics problem is solved for which the height of the platform z_0 is specified (i.e. the vertical component of the position of the platform`s origin in the base reference frame). The five unknowns of this problem are $x_0$, $y_0$, $\gamma_p$, $\theta_p$ and $\delta_p$. These are respectively the $x$ and $y$ components of the platform`s origin position in the base reference frame and the yaw, pitch and roll Euler angles describing the rotations necessary to go from the base reference frame to the platform reference frame. Let $\mathbf{p}_x$ and $\mathbf{p}_y$ be the unit vectors of the platform`s reference frame in plane with the platform and $\mathbf{g}_z$ be the gravity vector. Then the platform is considered levelled if the two following equations are respected:

$$\mathbf{p}_x \cdot \mathbf{g}_z = 0 \tag{1}$$
$$\mathbf{p}_y \cdot \mathbf{g}_z = 0. \tag{2}$$

Expanding these equations results in

$$\sin(\theta_n)\cos(\theta_p)\cos(\gamma_p) + \sin(\theta_p)\cos(\theta_n)\cos(\delta_n) - \sin(\delta_n)\sin(\gamma_p)\cos(\theta_n)\cos(\theta_p) = 0 \tag{3}$$

$$-\sin(\delta_p)\cos(\theta_n)\cos(\theta_p)\cos(\delta_n) - \sin(\theta_n)(\sin(\gamma_p)\cos(\delta_p) - \sin(\theta_p)\sin(\delta_p)\cos(\gamma_p)) - \sin(\delta_n)\cos(\theta_n)(\cos(\delta_p)\cos(\gamma_p) + \sin(\theta_p)\sin(\delta_p)\sin(\gamma_p)) = 0 \tag{4}$$

Where θ_n and δ_n are the pitch and roll angles of the base`s reference frame in the global reference frame. These two can be simply determined from the measurements of the accelerometer (a_x, a_y, a_z) mounted on the base as

$$\theta_n = \text{asin}\left(\frac{a_x}{\sqrt{(a_x)^2+(a_y)^2+(a_z)^2}}\right) \tag{5}$$

$$\delta_n = \text{asin}\left(-\frac{a_y}{\sqrt{(a_x)^2+(a_y)^2+(a_z)^2}}\cos^{-1}(\theta_n)\right) \tag{6}$$

Moreover, since each leg of the platform has a hinge pivot at the bottom, this means that the top attachment point of each leg can be viewed as constrained to a virtual plane fixed in the base reference frame. These describe three constraints which can be written as

$$\begin{gathered} y_0 + (0.5773503)L_p\sin(\gamma_p)\cos(\theta_p) \\ - H_p(\sin(\delta_p)\cos(\gamma_p) - \sin(\theta_p)\sin(\gamma_p)\cos(\delta_p)) = 0 \end{gathered} \tag{7}$$

$$\begin{gathered} (0.5)y_0 + (0.8660254)x_0 \\ + (0.25)L_p(\cos(\delta_p)\cos(\gamma_p) + \sin(\theta_p)\sin(\delta_p)\sin(\gamma_p)) \\ + (0.8660254)H_p(\sin(\delta_p)\sin(\gamma_p) + \sin(\theta_p)\cos(\delta_p)\cos(\gamma_p)) \\ - (0.25)L_p\cos(\theta_p)\cos(\gamma_p) - (0.1443376)L_p\sin(\gamma_p)\cos(\theta_p) \\ - (0.5)H_p(\sin(\delta_p)\cos(\gamma_p) - \sin(\theta_p)\sin(\gamma_p)\cos(\delta_p)) \\ - (0.4330127)L_p(\sin(\gamma_p)\cos(\delta_p) - \sin(\theta_p)\sin(\delta_p)\cos(\gamma_p)) = 0 \end{gathered} \tag{8}$$

$$\begin{gathered} (0.8660254)x_0 + (0.1443376)L_p\sin(\gamma_p)\cos(\theta_p) \\ + (0.25)\text{Lp}(\cos(\delta_p)\cos(\gamma_p) + \sin(\theta_p)\sin(\delta_p)\sin(\gamma_p) + (0.8660254)H_p(\sin(\delta_p)\sin(\gamma_p) + \sin(\theta_p)\cos(\delta_p)\cos(\gamma_p)) \\ + (0.4330127)L_p(\sin(\gamma_p)\cos(\delta_p)-\sin(\theta_p)\sin(\delta_p)\cos(\gamma_p)) + 0.5H_p(\sin(\delta_p)\cos(\gamma_p) \\ - \sin(\theta_p)\sin(\gamma_p)\cos(\delta_p)) - 0.5y_0 - 0.25L_p\cos(\theta_p)\cos(\gamma_p) = 0 \end{gathered} \tag{9}$$

Finally, from equations (3), (4), (7), (8) and (9), one can solve for the 5 unknowns (x_0, y_0, γ_p, θ_p and δ_p). Finding an algebraic solution to this system of nonlinear equations is however nontrivial: instead, a numerical approximation is used. Recovering the desired leg lengths (l_{1d}, l_{2d} and l_{3d}) once the position and orientation of the top platform is known is trivial. However, note that the initial choice for z_0 was arbitrary. To obtain leg lengths that guarantee the platform to be in its lowest position, only the index $i \in \{1,2,3\}$ of the shortest desired leg length is kept. A second inverse kinematics problem is then solved where instead of specifying the height of the platform z_0, the length of the leg with index i is specified such that this leg is completely retracted. Results from this second inverse kinematics problem are the desired leg lengths such that the platform is always at its lowest possible position, thus minimizing the height of the center of gravity of the system.

In order to monitor the progress of a leveling task, it is important for the operator to visualize the state of the platform (x_0, y_0, z_0, γ_p, θ_p, δ_p) given the current leg lengths as measured by the linear actuators' encoders (l_1, l_2, l_3). The general pathway for this forward kinematics problem is also shown in Figure 14. First, one should note that constraints (7), (8) and (9) are still active. Moreover, from the geometry of the problem, one can also derive expressions relating leg lengths (l_1, l_2, l_3) to position and orientation of the base and platform, leading to 3 additional independent equations:

$$\begin{gathered} (l_1)^2 + (2/3)L_p\cos(\theta_p)\cos(\gamma_p)(L_n-1.732051x_0) \\ + 2H_p\cos(\theta_p)\cos(\delta_p)(H_n-z_0) + 2H_py_0(\sin(\delta_p)\cos(\gamma_p) - \sin(\theta_p)\sin(\gamma_p)\cos(\delta_p)) \\ + (1.154701)H_p(L_n-(1.732051)x_0)(\sin(\delta_p)\sin(\gamma_p) + \sin(\theta_p)\cos(\delta_p)\cos(\gamma_p)) \\ - (H_p)^2 - 1/3(L_p)^2 - (y_0)^2 - (H_n - z_0)^2 - (1/3)(L_n-1.732051\,x_0)^2 \\ -(1.154701)L_py_0\sin(\gamma_p)\cos(\theta_p) - 1.154701)L_p\sin(\theta_p)(H_n-z_0) = 0 \end{gathered} \tag{10}$$

$$\begin{gathered} (l_2)^2 + (0.5773503)L_p\sin(\theta_p)(H_n-z_0) + L_p\sin(\delta_p)\cos(\theta_p)(H_n-z_0) \\ +(0.1666667)L_p\cos(\theta_p)\cos(\gamma_p)(L_n+(3.464102)x_0) \\ +2H_p\cos(\theta_p)\cos(\delta_p)(H_n-z_0) + 0.5L_p(L_n-2y_0)(\cos(\delta_p)*\cos(\gamma_p) + \sin(\theta_p)\sin(\delta_p)\sin(\gamma_p)) \\ +(0.2886751)L_p(L_n+(3.464102)x_0)(\sin(\gamma_p)\cos(\delta_p) - \sin(\theta_p)\sin(\delta_p)\cos(\gamma_p)) - (H_p)^2 - 1/3(L_p)^2 \\ - (H_n-z_0)^2 - 1/4(L_n-2y_0)^2 - 0.08333333(L_n+(3.464102)x_0)^2 - (0.2886751)L_p\sin(\gamma_p)\cos(\theta_p)(L_n-2y_0) \\ - (0.5773503)H_p(L_n+(3.464102)x_0)(\sin(\delta_p)\sin(\gamma_p) + \sin(\theta_p)\cos(\gamma_p)\cos(\gamma_p)) \\ - H_p(L_n-2y_0)(\sin(\delta_p)*\cos(\gamma_p)-\sin(\theta_p)\sin(\gamma_p)\cos(\delta_p)) = 0 \end{gathered} \tag{11}$$

$$
\begin{aligned}
&(l_3)^2 + (0.5773503)L_p\sin(\theta_p)(H_n - z_0) \\
&+(0.1666667)L_p\cos(\theta_p)\cos(\gamma_p)(L_n+(3.464102)x_0) \\
&+ (0.2886751)L_p\sin(\gamma_p)\cos(\theta_p)(L_n+2y_0) + 2H_p\cos(\theta_p)\cos(\delta_p)(H_n - z_0) \\
&+ (0.5)\mathrm{Lp}(L_n+2y_0)(\cos(\delta_p)\cos(\gamma_p)+\sin(\theta_p)\sin(\delta_p)\sin(\gamma_p)) \\
&+H_p(L_n+2y_0)(\sin(\delta_p)\cos(\gamma_p) - \sin(\theta_p)\sin(\gamma_p)\cos(\delta_p)) \\
&- (H_p)^2 - (1/3)(L_p)^2 - (H_n - z_0)^2 - (0.25)(L_n+2y_0)^2 \\
&- 0.08333333(L_n+(3.464102)x_0)^2 - L_p\sin(\delta_p)\cos(\theta_p)(H_n - z_0) \\
&- 0.5773503(H_p)(L_n+ (3.464102)x_0)(\sin(\delta_p)\sin(\gamma_p) + \sin(\theta_p)\cos(\delta_p)\cos(\gamma_p)) \\
&-(0.2886751)L_p(L_n+ (3.464102)x_0)(\sin(\gamma_p)\cos(\delta_p) - \sin(\theta_p)\sin(\delta_p)\cos(\gamma_p)) = 0
\end{aligned}
\tag{12}
$$

where the definition of all the known constants are included in Table 4. Finally, numerical methods can once again be used to solve the system of six nonlinear equations formed by equations (7)-(12) to obtain the current state captured by the six variables x_0, y_0, z_0, γ_p, θ_p, δ_p.

Table. 4 Constants Describing the Geometry of the Leveler Platform

Constants	Definition
L_p	Distance between leg top attachment points on platform (assumed same between all adj. attachment points)
L_n	Distance between leg bottom attachment points on base (assumed same between all adj. attachment points)
H_p	Vertical offset between each of the leg top attachment points and the origin of the platform reference frame
H_n	Vertical offset between each of the leg bottom attachment points and the origin of the base reference frame

Appendix B

Table. 5 Mass budget by subsystem. Margins are accounted for within each subsystem.

Subsystem	% of Budget	Mass (kg)	Sources
Payload	11.29%	2.85	Platform structure, motor, radio and camera payloads, solar panels & battery, miscellaneous electronics.
Composite Boom	3.17%	0.8	
Deployer	49.50%	12.5	Housing structure, motor, bearings, puller.
Leveler	36.04%	9.1	3 linear actuators, structure, miscellaneous electronics.
Total	**100%**	**25.25**	

Table. 6 Risk analysis and mitigation by subsystem.

ID	Subsystem	Risk Description	Mitigation Strategy	Likelihood	Impact
L01	Leveler	Leveler angle cannot be adjusted	Test the range of leveling with only one/two motors working	1	3
L02	Leveler	Leveler angle cannot be detected		1	3
L03	Leveler	Less power is provided than needed, or no power is provided at all	Have a backup power source (may not be feasible)	1	5
L04	Leveler	Leveler can't hold load	Test leveler at loads above expected with a significant safety factor, i.e. 2	1	5
L05	Leveler			2	2
L06	Leveler	Action not triggered by main computer, or MELLTT can't send data about its orientation	Have a backup command method	1	5
L07	Leveler		Have a backup locking mechanism	2	5
L08	Leveler	Leveler partially completes required level, but not to full extent, i.e. levels 6 degrees when 12 was needed		2	3
P01	Payload	There is a probability that, if any component shifts during deployment, the loads on the upper bus might become unbalanced and exert a moment load on the boom, causing tipping or buckling.	Test forces during deployment and secure components to withstand deployment loads.	1	5
P02	Payload	If the pointing module produces vibration near the natural frequencies of the boom, then there is a risk that excessive vibration will cause failure in the boom.	Test and reduce the speed at which the upper bus rotates if necessary.	2	4
P03	Payload	Data transmission stops insufficient power, issues with connectivity, etc.	Have semi-continuous transmission rather than block transmission (e.g. transmit data as/ right after they are gathered rather than in a single batch at predetermined intervals).	1	5

ID	Subsystem	Risk Description	Mitigation Strategy	Likelihood	Impact
D01	Deployer	Power is not (fully) delivered to deployer.	Have backup power source. Identify minimum power requirement.	1	4
D02	Deployer	Deployer is unable to support load.	Test deployment of excess load.	1	5
D03	Deployer	Essential deployer structure (bracing, etc) is damaged during transit or while deployment.	Have redundant or backup components for especially sketchy parts.	2	5
D04	Deployer	Motor does not provide sufficient torque for deployment.	Identify methods of motor failure (ex: failure due to insufficient power, broken bearing, etc) and come up with individual mitigation plans (ex: see mitigation for D01, have backup part, etc).	1	5
D05	Deployer	Deployer deploys partly, but not to full intended height.	Add stabilization features that stabilizes sections of the boom as it deploys, decreasing the amount of boom in unstabilized states.	2	4
D06	Deployer	Deployer fails to stop and lock when boom fully deploys.	See D06. Add feature to physically or electronically constrain deployment after boom is (expected to be) fully deployed. Have kill switch for motor.	2	4
D07	Deployer	Deployment not triggered/ stopped by computer.	Have manual command method as backup.	1	4
D08	Deployer	Deployer-leveler interface detaches during transit.	Conduct vibrational tests. Be able to reattach interface.	1	4
D09	Deployer	Deployer-payload interface detaches during transit.	Conduct vibrational tests. Be able to reattach interface.	1	4
D10	Deployer	Deployer-payload interface fails to separate during boom deployment.	Ensure deployer and boom are not damaged in the case of a failure to separate. Worst case scenario, use kill switch for motor and separate by hand.	1	4
B01	Boom	Test with incremental loading, from 0 to an excess load for a safety factor.	Test with incremental loading, from 0 to an excess load for a safety factor.	1	5
B02	Boom	Slow motor speed for deployment/ payload movement. Add damping mechanisms.	Slow motor speed for deployment/ payload movement. Add damping mechanisms.	2	4
B03	Boom	During deployment, boom uncoils rather than extend, causing a failure to deploy.	Add feature to prevent blossoming.	3	5
B04	Boom	Conduct vibrational tests. Be able to reattach interface.	Conduct vibrational tests. Be able to reattach interface.	1	5

Acknowledgments

The authors would like to thank the National Institute of Aerospace, NASA's Space Technology Mission Directorate and Massachusetts Space Grant for funding support; the NASA Langley Deployable Composite Booms Team and FormLabs for in-kind support and MIT's Department of Aeronautics and Astronautics for access to facilities and services. Mentorship, advice and/or feedback from BIG Idea Judges, NASA Langley, NASA Kennedy Space Center, Jet Propulsion Laboratory and Robots5, LLC was invaluable to the development of our design.

References

[1] NASA's Breakthrough Innovative and Game-changing (BIG) Idea Challenge, "2020 Lunar PSR Challenge Details," National Institute of Aerospace, 2020. [Online]. Available: https://bigidea.nianet.org/competition-basics/. [Accessed: 27-Sep-2020].

[2] Astrobotic, "Peregrine Lunar Lander Payload User's Guide Version 3.2," Jun. 2019.

[3] National Aeronautics and Space Administration, "NASA Technology Readiness Levels." [Online]. Available: https://www.nasa.gov/sites/default/files/trl.png. [Accessed: 27-Sep-2020].

[4] Fernandez, J et. al. An Advanced Composites-Based Solar Sail System for Interplanetary Small Satellite Missions, AIAA Spacecraft Structures Conference. 2018

[5] Reveles, JR et al. In-Orbit Performance of AstroTube: AlSat Nano's Low Mass Deployable Composite Boom Payload, SmallSat Conference. 2017

[6] M. Faessler, E. Mueggler, K. Schwabe and D. Scaramuzza, "A monocular pose estimation system based on infrared LEDs," 2014 IEEE International Conference on Robotics and Automation (ICRA), Hong Kong, 2014, pp. 907-913, doi: 10.1109/ICRA.2014.6906962.

[7] R. Johanson, D. Jang, E. Kononov, M. Luu, S. Morgan, J. Todd, M. Blevins, M. Contreras, D. Erkel, A. Garcia, J. Holland, A. Kharsansky, B. Martell, A. Mitchell, T. Roberts, J. Schultz, A. Sentis, J. Rockaway and J. A. Hoffman, "What could we do with a 20-meter tower on the Lunar South Pole? Applications of the Multifunctional Expandable Lunar Lightweight, Tall Tower (MELLTT)", 2020 ASCEND Conference, Las Vegas, submitted for publication